

A Compact Ultrawideband Circularly Polarized Antenna Array With Shared Partial Patches

Wei He , Yejun He , Senior Member, IEEE, Yin Li , Sai-Wai Wong , Senior Member, IEEE, and Lei Zhu , Fellow, IEEE

Abstract—In this letter, a compact ultrawideband circularly polarized (CP) antenna array is proposed. The antenna array consists of four cross dipoles with asymmetric elliptical arms and a wideband 1-to-4 feeding network. By employing the ellipses of different sizes as the arms of the cross dipole, the operating bandwidth of the antenna array element can be enhanced. Rotating four of these elements in sequence can obtain an antenna array with symmetrical radiation patterns. The size of the antenna array can be reduced by shortening the distance between adjacent elements and exchanging the upper and lower layers patches of the second and fourth elements to partially overlap between adjacent elements. In addition, the axial ratio (AR) bandwidth can be further expanded because of the sequential rotation topology and the wideband feeding network with a 90° phase difference between adjacent elements. A prototype is fabricated to verify the design principle. The measured and simulation results show that the proposed antenna array has great CP characteristics. The measured impedance bandwidth for $|S_{11}| < -10 \text{ dB}$ and 3 dB AR bandwidth are about 104.4% and 111.8%, respectively. The peak gain is 13.2 dBic at 4.5 GHz. The overall size of the antenna array is only $0.88 \lambda \times 0.88 \lambda \times 0.14 \lambda$ (λ refers to the wavelength of the lowest operating frequency in free space).

Index Terms—Circularly polarized (CP) antenna, cross dipole, ultrawideband antenna.

I. INTRODUCTION

IN RECENT years, more and more ultrawideband (UWB) antennas have been widely used in indoor and outdoor positioning, radar imaging, wireless data collection, and other wireless communication systems [1]. As multifunctional systems and miniaturized systems become more and more popular, the demand for UWB antennas with compact and circular polarization (CP) is also increasing.

Manuscript received May 25, 2021; revised June 25, 2021 and July 27, 2021; accepted July 29, 2021. Date of publication August 24, 2021; date of current version December 20, 2021. This work was supported in part by the National Natural Science Foundation of China under Grant 62171306, Grant 61801299, Grant 61871433, and Grant 61828103; in part by Shenzhen Science and Technology Program under Grant GJHZ20180418190529516, Grant JSGG20180507183215520, and Grant JCYJ20200109113601723; in part by the Natural Science Foundation of Guangdong Province under Grant 2018A0303130141; and in part by the Natural Science Foundation of Hunan Province under Grant 2021JJ50082. (Corresponding author: Yin Li.)

Wei He is with the School of Electrical and Information Engineering, Hunan Institute of Technology, Hengyang 421002, China (e-mail: hewei21801@163.com).

Yejun He, Yin Li, and Sai-Wai Wong are with the College of Electronics and Information Engineering, Shenzhen University, Shenzhen 518060, China (e-mail: heyejun@126.com; liyinuestc@gmail.com; wongsaiwai@ieee.org).

Lei Zhu is with the Department of Electrical and Computer Engineering, University of Macau (UM), Taipa 999078, Macau (e-mail: leizhu@um.edu.mo). Digital Object Identifier 10.1109/LAWP.2021.3107218

A variety of different wideband and UWB CP antennas have been reported. A CP dielectric resonator antenna loaded with the partially reflective surface could achieve a wide axial ratio (AR) bandwidth of 54.9%, while it has a higher profile (0.6λ) [2]. A compact CP spiral antenna was proposed in [3], and its AR bandwidth covered the frequency range of 2–6 GHz. By using a pair of curved tapered slots with a meshed reflector to obtain an UWB antenna and employing double Y-shaped slots with a multilayer patch to achieve an UWB high gain antenna were described in [4] and [5], respectively. In [6], an L-shaped radiator monopole antenna with defect ground was illustrated, the AR bandwidth was about 115.2%; an UWB CP antenna consisting of an asymmetric-fed radiator and a frame structure lower ground with an U-shaped slot was shown in [7], the AR bandwidth of about 110.5%; and in [8], a geometrically simple compact UWB CP antenna was proposed, it exhibits an AR bandwidth of about 82%, but these antennas were with bidirectional radiations. An UWB CP asymmetric-S antenna with the AR bandwidth of about 84.8% was presented in [9], its overall size was $1.07 \lambda \times 1.07 \lambda \times 0.36 \lambda$. In addition, a cross dipole antenna with ellipse arms that could reach a 3 dB AR bandwidth of about 96.6% from 1 to 2.87 GHz was illustrated in [10], and adding four rotated elliptical slots to the elliptical arms could obtain 4.1:1 AR bandwidth [11]. The antennas mentioned previously are all different types of UWB CP antennas realized by a single feed, but the use of multifeed technology can achieve a compact UWB CP antenna. A compact UWB CP antenna based on crossed tapered slot radiation elements was mentioned in [12], its 3 dB axial ratio bandwidth is 105.5%, but it has a complicated 3-D structure. In [13], a multimode patch antenna with a four-feed network was illustrated, the AR bandwidth of which was 85%. Nevertheless, the gain of which is only 6 dBic. In [14], four broadband CP monopole elements with a sequentially rotated feeding network are used to excite the UWB CP radiation, but this antenna has a complicated gradient artificial magnetic conductor with a metal cone. A 2×2 sequentially rotated symmetric metasurface antenna with a slot linear polarized antenna array could achieve a 3 dB AR bandwidth of about 83.2% [15], but this antenna could not maintain a stable and symmetrical radiation pattern in the operating frequency bandwidth. In a word, the antennas mentioned previously are either thick in profile, large in size, or have narrow bandwidth.

In this letter, we proposed a compact UWB CP antenna array with shared partial patches. The proposed antenna array consists of two-layer printed circuit boards (PCBs). Four cross dipoles

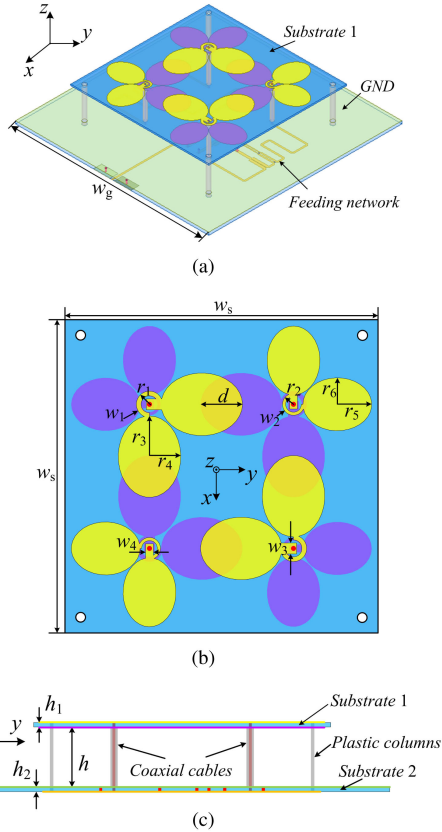


Fig. 1. Configuration of the proposed antenna array. (a) 3-D view. (b) Top view of 2×2 antenna arrangement. (c) Side view.

with asymmetric elliptical arms are printed on the two sides of the top PCB, and a wideband 1-to-4 feeding network is printed on the bottom PCB. Using ellipses of different sizes as the arms of the cross dipole, the operating bandwidth of the antenna array element can be enhanced. By shortening the distance between adjacent elements and exchanging the upper and lower layers patches of the second and fourth elements to partially overlap between adjacent elements can reduce the size of the antenna array. In addition, the sequential rotation topology and the wideband feeding network can further enhance the AR bandwidth. The simulated and measured results verify the good performance of the proposed antenna array.

II. ANTENNA DESIGN AND ANALYSIS

Fig. 1 shows the configuration of the proposed antenna array, which consists of 2×2 sequentially rotated cross dipoles with asymmetric elliptical arms, a feeding network, two layers of substrate, four supporting plastic columns, and four feeding coaxial cables. The top layer substrate ($\epsilon_1 = 2.2$ and $\tan \delta_1 = 0.0009$) has a size of $w_s \times w_s$ and a thickness of h_1 (0.508 mm). Four cross dipoles with asymmetric elliptical arms are printed on the two sides of the substrate. By using the ellipses of different sizes as the arms of the cross dipole, the operating bandwidth of the antenna array element can be enhanced. As shown in Fig. 1(b), the size of the proposed antenna array can be reduced by exchanging the upper and lower patches of adjacent antenna array elements and overlapping partial patches of the

TABLE I
ANTENNA PARAMETERS (mm)

w_1	w_2	w_3	w_4	w_s	w_g	d	h
1.5	1	3.5	2.5	100	140	13.4	22
r_1	r_2	r_3	r_4	r_5	r_6	h_1	h_2
4.2	3.5	13	10	11	8.5	0.508	0.508

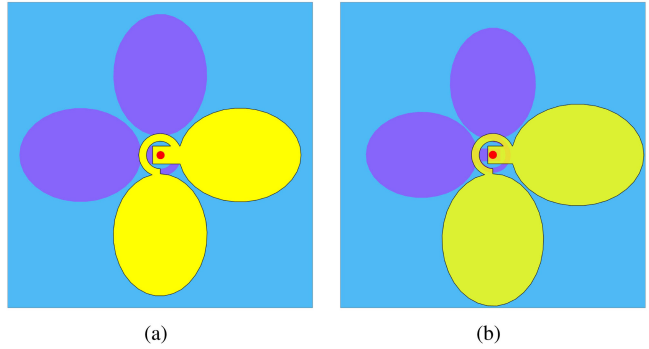


Fig. 2. (a) Reference antenna. (b) Proposed antenna element.

adjacent antenna array elements simultaneously. The width of the overlapped part is d (13.4 mm). In addition, this special topology structure shown in Fig. 1 can enable the antenna array to obtain a stable and symmetrical radiation pattern. More importantly, compared with the conventional array, this topology structure makes the distance between antenna elements only 46 mm, much less than the half of the free-space wavelength at 1.9 GHz (78.9 mm). Furthermore, when a wideband feeding network with a 90° phase difference between adjacent elements is added, the operating bandwidth of the proposed antenna array can be greatly expanded. The optimized design parameters are as follows in Table I.

To illustrate the advantages of the proposed design method, the cross dipole with symmetric elliptical arms and the conventional array composed of those are compared with the proposed antenna element and array. The geometries of the cross dipole with symmetric elliptical arms (reference antenna) and asymmetric elliptical arms (proposed antenna element) are shown in Fig. 2. As shown, one half of the proposed antenna element is slightly smaller than the cross dipole with symmetric elliptical, while the other half is slightly larger than the cross dipole with symmetric elliptical. The performance comparison of the two antennas for $|S_{11}|$, and AR and gain are shown in Fig. 3(a) and (b), respectively. It can be seen that the impedance bandwidth of the two antenna is almost consistent, while the 3 dB AR bandwidth of the proposed antenna element is much wider. This is because slightly reducing the half of the cross dipole with symmetrical elliptical arms will extend the operating frequency to a higher frequency, while slightly increasing the size of the other half will extend the operating frequency to a lower frequency. In short, selecting the size of the asymmetric elliptical arms of the cross dipole properly can obtain a wider operating bandwidth.

As shown in Fig. 4(a), the feeding network is printed on the bottom layer substrate. The bottom layer substrate ($\epsilon_2 = 3.55$

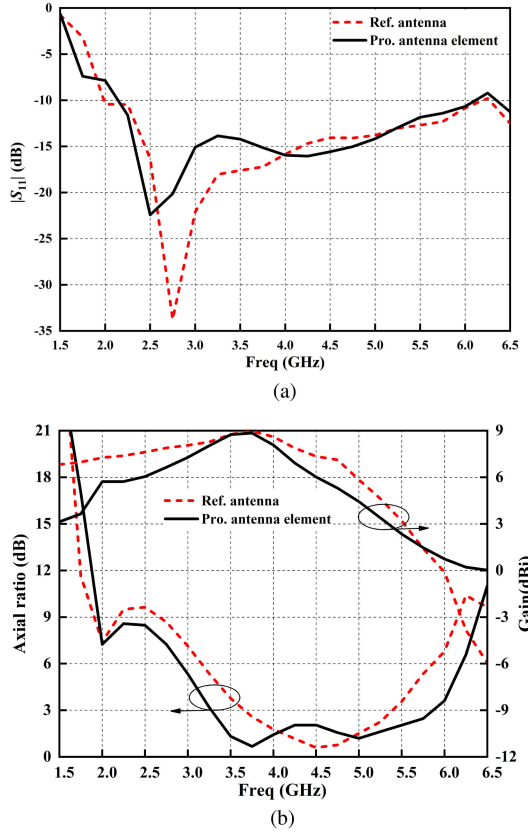


Fig. 3. $|S_{11}|$ and AR of the reference antenna and the proposed antenna element. (a) $|S_{11}|$. (b) AR and gain.

and $\tan \delta_1 = 0.0027$) has a size of $w_g \times w_g$ and a thickness of h_2 (0.508 mm). This feeding network has an UWB power divider and a stable phase difference performance and consists of a 180° out-of-phase balun and two 90° baluns, which is designed in [16]. The simulation results of this feeding network are illustrated in Fig. 4(b). The impedance bandwidth of the feeding network with $|S_{11}| < -10$ dB is from 1.82 to 6.21 GHz (109.3%), and the phase difference between Port 2, Port 3, Port 4, and Port 5 is maintained at about 90° within the bandwidth of 1.82–6.21 GHz. The magnitude unbalance of the insertion loss is less than 1.5 dB.

III. RESULTS AND DISCUSSIONS

To prove the correctness of the previous analysis, the proposed compact UWB CP antenna array was fabricated and measured. The photos of the fabricated antenna are shown in Fig. 5. The simulated and measured results of the proposed antenna array in terms of S-parameters, AR, and gain performance are shown in Figs. 6 and 7, respectively. As shown in Fig. 6, the measured impedance bandwidth of $|S_{11}| < -10$ dB is about 104.4% (3.18:1, 1.96–6.24 GHz), which is in a good agreement with the simulated result. As illustrated in Fig. 7, the measured 3 dB AR bandwidth can cover the frequency range from 1.75 to 6.19 GHz, reaching 111.8% (3.53:1), which is slightly different from the simulated result. In addition, the measured gain is positive in the operating bandwidth, a slight fluctuation compared with the

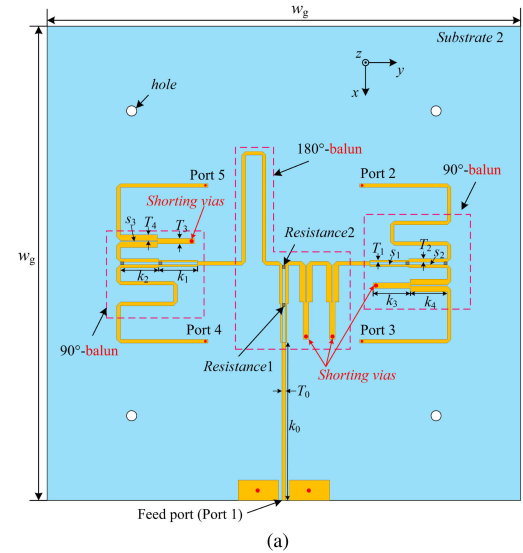


Fig. 4. Feeding network of the proposed antenna array. (a) Schematic of the feeding network. (b) Simulation performance of the feeding network. ($w_g = 140$ mm, $k_0 = 46.65$, $k_1 = 11.5$, $k_2 = 11.3$, $k_3 = 10.9$, $k_4 = 11$, $T_0 = 1.1$, $T_1 = 0.53$, $T_2 = 0.96$, $T_3 = 1.74$, $T_4 = 1.65$, $s_1 = 0.8$, $s_2 = 0.8$, $s_3 = 0.3$ mm, $Resistance1 = 62 \Omega$, and $Resistance2 = 562 \Omega$.)

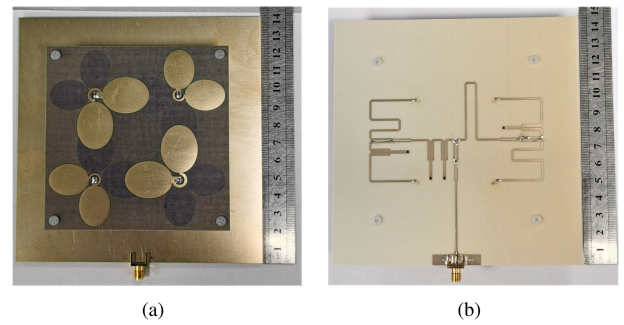


Fig. 5. Prototype of the proposed antenna. (a) Top view. (b) Bottom view.

simulated gain, and the peak gain is 13.2 dBi at 4.25 GHz. The measured and simulated results of the radiation pattern in the xoz and yoz planes at 2.5, 3.5, 4.5, and 5.5 GHz are plotted in Fig. 8(a)–(d), respectively. The antenna yields a stable left-hand CP radiation pattern in both xoz and yoz planes at all frequencies. The performance comparison between the proposed

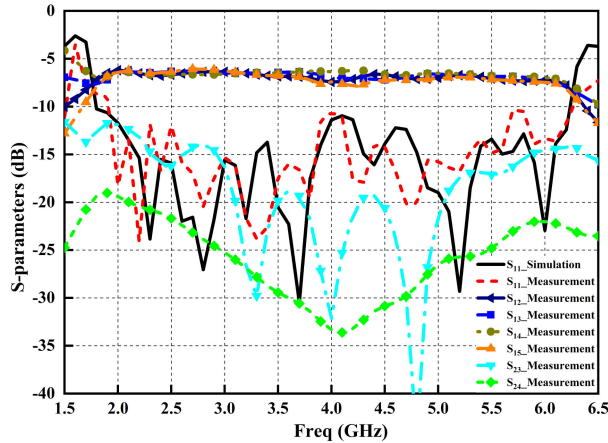


Fig. 6. Simulated and measured S-parameters of the proposed antenna.

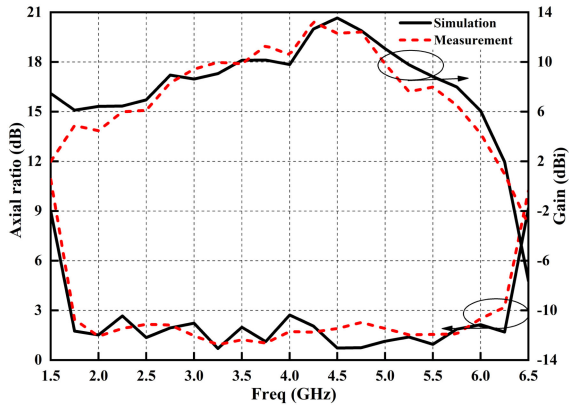


Fig. 7. Simulated and measured AR and gain of the proposed antenna.

TABLE II
COMPARISON BETWEEN THE PROPOSED ANTENNA AND
OTHER UWB CP ANTENNA

Ref.	Antenna Size (λ^3/mm^3)	Impedance bandwidth	AR bandwidth	Peak gain (dBi)
[12]	$0.33\lambda \times 0.33\lambda \times 0.3\lambda$ $53 \times 53 \times 47$	108% 1.85-6.22 GHz	107% 1.82-6.2 GHz	8
[13]	$0.62\lambda \times 0.62\lambda \times 0.1\lambda$ $85 \times 85 \times 8.5$	85% 2.2-5.5 GHz	85% 2.2-5.5 GHz	6
[14]	$1.17\lambda \times 1.17\lambda \times 0.1\lambda$ $200 \times 200 \times 17.5$	132.8% 1.17-5.79 GHz	92.5% 1.75-4.76 GHz	12.6
[15]	$0.8\lambda \times 0.8\lambda \times 0.05\lambda$ $77 \times 77 \times 4.38$	97.2% 2.75-7.95 GHz	83.2% 3.3-7.75 GHz	10.8
[16]	$1.13\lambda \times 1.13\lambda \times 0.15\lambda$ $85 \times 85 \times 11.6$	98% 2.5-9.2 GHz	96.3% 2.15-6 GHz	9.5
This work	$0.88\lambda \times 0.88\lambda \times 0.14\lambda$ $140 \times 140 \times 23$	104.4% 1.96-6.24 GHz	111.8% 1.75-6.19 GHz	13.2

antenna array and other UWB CP arrays is shown in Table II. It can be shown that the proposed antenna not only has a compact size but also has a wider 3 dB AR bandwidth.

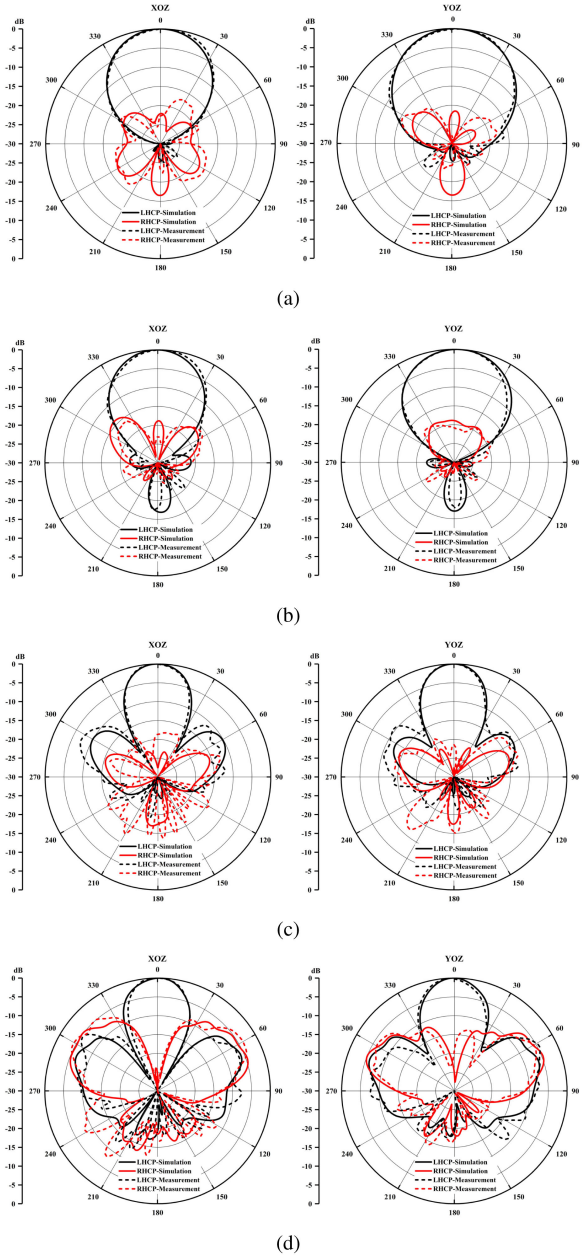


Fig. 8. Simulated and measured radiation pattern of the proposed antenna in xoz and yoz planes. (a) 2.5 GHz. (b) 3.5 GHz. (c) 4.5 GHz. (d) 5.5 GHz.

IV. CONCLUSION

In this letter, a compact UWB CP array with shared partial patches is proposed. By using an asymmetric ellipse to replace the arms of the conventional cross dipole, the operating bandwidth can be enhanced. Rotating four of these elements in a sequence and exchanging the upper and lower patches of adjacent antenna array elements and making the adjacent antenna array elements partially overlapped can reduce the size of the proposed antenna array. The overall size of the antenna array is only $0.88\lambda \times 0.88\lambda \times 0.14\lambda$. In addition, the impedance bandwidth of 104.4% and AR bandwidth of 111.8% are mentioned. The good performance of this antenna array makes it a potential candidate for many UWB applications.

REFERENCES

- [1] Y. Qi, B. Yuan, Y. Cao, and G. Wang, "An ultrawideband low-profile high-efficiency indoor antenna," *IEEE Antennas Wireless Propag. Lett.*, vol. 19, no. 2, pp. 346–349, Feb. 2020.
- [2] J. Wen, Y. C. Jiao, Y. X. Zhang, and J. Jia, "Wideband circularly polarized dielectric resonator antenna loaded with partially reflective surface," *Int. J. RF Microw. Comput.-Aided Eng.*, vol. 29, no. 12, pp. e21962.1–e21962.9, Aug. 2019.
- [3] Y. Zhong, G. Yang, J. Mo, and L. Zheng, "Compact circularly polarized archimedean spiral antenna for ultrawideband communication applications," *IEEE Antennas Wireless Propag. Lett.*, vol. 16, pp. 129–132, 2017.
- [4] Y. Pan and Y. Dong, "Low-profile low-cost ultrawideband circularly polarized slot antennas," *IEEE Access*, vol. 7, pp. 160 696–160 704, 2019.
- [5] J. Wei, X. Jiang, and L. Peng, "Ultrawideband and high-gain circularly polarized antenna with double-Y-shape slot," *IEEE Antennas Wireless Propag. Lett.*, vol. 16, pp. 1508–1511, 2017.
- [6] R. Xu, J. Li, J. Liu, S. G. Zhou, and K. Wei, "UWB circularly polarised slot antenna with modified ground plane and L-shaped radiator," *Electron. Lett.*, vol. 54, no. 15, pp. 918–920, Jul. 2018.
- [7] R. Xu, J. Li, J. Yang, K. Wei, and Y. Qi, "A design of U-shaped slot antenna with broadband dual circularly polarized radiation," in *IEEE Trans. Antennas and Propagation*, vol. 65, no. 6, pp. 3217–3220, Jun. 2017.
- [8] U. Ullah, S. Koziel, and I. B. Mabrouk, "A simple-topology compact broadband circularly polarized antenna with unidirectional radiation pattern," *IEEE Antennas and Wireless Propagation Letters*, vol. 18, no. 12, pp. 2612–2616, Dec. 2019.
- [9] W. He *et al.*, "An ultrawideband circularly polarized asymmetric-S antenna with enhanced bandwidth and beamwidth performance," *IEEE Access*, vol. 7, pp. 134895–134902, 2019, doi: [10.1109/ACCESS.2019.2941551](https://doi.org/10.1109/ACCESS.2019.2941551).
- [10] L. Zhang *et al.*, "Single-feed ultrawideband circularly polarized antenna with enhanced front-to-back ratio," *IEEE Trans. Antennas Propag.*, vol. 64, no. 1, pp. 355–360, Jan. 2016.
- [11] A. Akbarpour and S. Chamaani, "Ultrawideband circularly polarized antenna for near-field SAR imaging applications," *IEEE Trans. Antennas Propag.*, vol. 68, no. 6, pp. 4218–4228, Jun. 2020.
- [12] X. Ding, Z. Zhao, Y. Yang, Z. Nie, and Q. H. Liu, "A compact unidirectional ultrawideband circularly polarized antenna based on crossed tapered slot radiation elements," *IEEE Trans. Antennas Propag.*, vol. 66, no. 12, pp. 7353–7358, Dec. 2018.
- [13] C. Sun, "A design of compact ultrawideband circularly polarized microstrip patch antenna," *IEEE Trans. Antennas Propag.*, vol. 67, no. 9, pp. 6170–6175, Sep. 2019.
- [14] R. Xu *et al.*, "Analysis and design of ultrawideband circularly polarized antenna and array," *IEEE Trans. Antennas Propag.*, vol. 68, no. 12, pp. 7842–7853, Dec. 2020.
- [15] L. Gu, W. Yang, W. Feng, Q. Xue, Q. Meng, and W. Che, "Low-profile ultrawideband circularly polarized metasurface antenna array," *IEEE Antennas Wireless Propag. Lett.*, vol. 19, no. 10, pp. 1714–1718, Oct. 2020.
- [16] Q. Liu, Z. N. Chen, Y. Liu, and C. Li, "Compact ultrawideband circularly polarized weakly coupled patch array antenna," *IEEE Trans. Antennas Propag.*, vol. 65, no. 4, pp. 2129–2134, Apr. 2017.